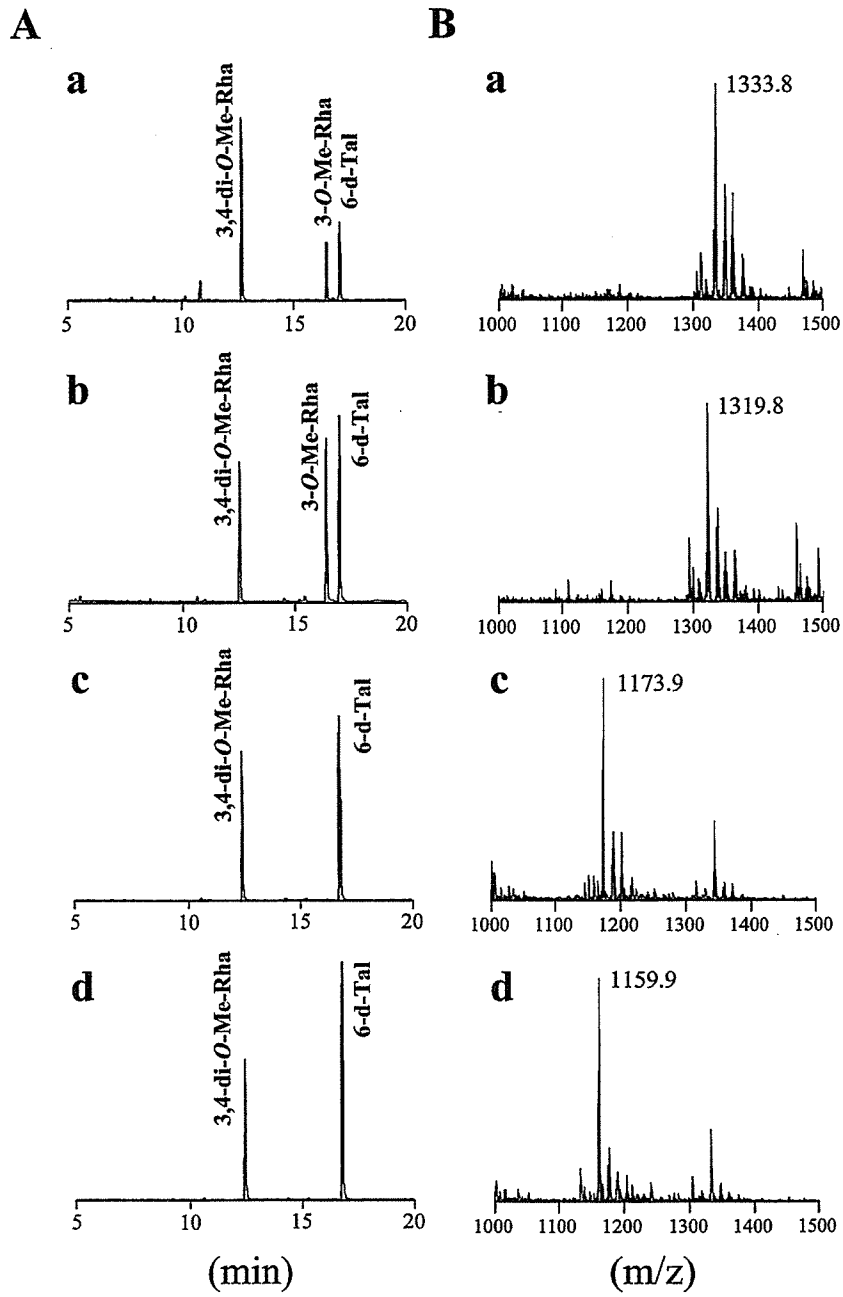

FIG. 4. Biochemical characterization of GPL-5 (a), GPL-6 (b), GPL-3 (c), and GPL-4 (d). (A) GC/MS analysis of alditol acetates of sugars released from each purified GPL. (B) MALDI-TOF/MS analysis of total molecular mass of each purified GPLs. (C) MALDI-TOF/MS analysis of total molecular mass of purified GPL-5 (a) and GPL-6 (b), which were subjected to β-elimination.

GPL-6 were *m/z* 1,171.7 and 1,157.7, respectively, which resulted in the loss of total mass of 162, suggesting that 6-d-Tal was linked to the position of D-*allo*-Thr (Fig. 4C). The linkage position of the sugars linked to the L-alaninol site of GPL-5 and GPL-6 was then determined by GC/MS analyses followed by perdeuteriomethylation. As shown in Fig. 5A, the GC profiles of alditol acetates from perdeuteriomethylated GPL-5 gave three peaks corresponding to 6-d-Tal, 3-*O*-Me-Rha, and 3,4-di-*O*-Me-Rha. The characteristic spectra of 3-*O*-Me-Rha and 3,4-di-*O*-Me-Rha, which are predicted to be linked to L-alaninol, are illustrated in Fig. 5B and C, respectively. The spectrum of 3-*O*-Me-Rha gave fragment ions at *m/z* 121, 134, and 165, which represent the presence of a deuteriomethyl group at positions C-2 and C-4. In contrast, no deuteriomethyl group was observed in 3,4-di-*O*-Me-Rha, whose C-2 position was acetylated, supported by the detection of fragment ions at *m/z* 131 and 190. The results from GC/MS analyses of perdeuteriomethylated GPL-6 were the same as those for GPL-5 (not shown). These observations demonstrated that GPL-5 and GPL-6 have the same sugar moieties, which are 6-d-Tal at

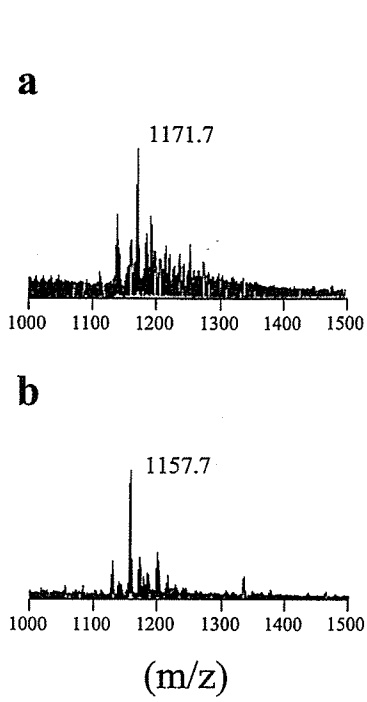

FIG. 4—*Continued.*

D-*allo*-Thr and 3-*O*-Me-rhamnosyl-(1→2)-3,4-di-*O*-Me-Rha at L-alaninol, indicating that 3-*O*-Me-Rha was linked to GPL-3 and GPL-4 (Fig. 6).

Overexpression of *gtf1*, *gtf2*, *gtf3*, and *gtf4* in *M. smegmatis* mc²155. To investigate the effects of overexpression of each gene on GPL biosynthesis, we constructed four *gtf*-overexpressed strains in wild-type mc²155 and compared the profile of total GPLs by TLC analyses. The results showed that the profiles of Wt/pMVgtf1, Wt/pMVgtf2, and Wt/pMVgtf4 were the same as that of Wt/pMV261, whereas Wt/pMVgtf3 produced two major compounds whose biochemical data corresponded to those of GPL-5 and GPL-6 (Fig. 7).

Characterization of *M. avium gtfA* and *gtfB*. We showed that both *M. smegmatis gtf1* and *gtf2* were responsible for glycosylation of the fatty acyl-tetrapeptide core. Comparison of the genome sequences encompassing the GPL biosynthetic gene cluster among several species of *M. avium* have shown that *gtfA* and *gtfB* (GenBank accession no. AF125999.1) are very similar to *M. smegmatis gtf1* and *gtf2*, respectively, in the corresponding putative amino acid sequences and might contribute to the glycosylation of the fatty acyl-tetrapeptide core (13). However, the function of each gene has not been thoroughly analyzed (13). Therefore, to confirm the role of *gtfA* and *gtfB*, we complemented Δgtf1 and Δgtf2 with the *gtf* expression vectors carrying *gtfA* (pMVgtfA) and *gtfB* (pMVgtfB). As shown in Fig. 8, TLC analyses revealed that *gtfA* and *gtfB* restored the production of wild-type GPLs in Δgtf1 and Δgtf2, respectively, whereas transformants with reverse vectors (Δgtf1/pMVgtfB and Δgtf2/pMVgtfA) did not produce wild-type GPLs. These results suggested that the function of *M. avium gtfA* and *gtfB* is the same as that of *M. smegmatis gtf1* and *gtf2*, respectively.

DISCUSSION

It has been shown that the *rtfA* gene of *M. avium* encodes a rhamnosyltransferase which synthesizes ssGPLs, while other genes involved in the glycosylation of the fatty acyl-tetrapeptide core remain unknown (12). In this study, we focused on the four genes of *M. smegmatis*, which show high similarity to *rtfA*, and generated their disruptants to characterize the role in the GPL biosynthesis.

In the early glycosylation steps of the fatty acyl-tetrapeptide core, we observed that the disruption of *gtf1* abolished the whole GPLs and led to the accumulation of *O*-Me-Rha derivatives without 6-d-Tal in Δgtf1 (Fig. 3B). Thus, we propose that the *gtf1* gene product catalyzes the transfer of 6-d-Tal to fatty acyl-tetrapeptide core. It is reported that the *M. avium* 104Rg strain, which has a spontaneous deletion in the genome region including *gtfA*, also accumulated *O*-methylated and nonmethylated Rha without 6-d-Tal (13, 30). This property is directly supported by our result that the *gtfA* could complement Δgtf1 (Fig. 8). However, *M. avium* 104Rg mainly contained nonmethylated Rha, whereas Δgtf1 derived from *M. smegmatis* mc²155 contained only *O*-Me-Rha. These different observations may be due to differences in the substrate specificity of methyltransferase, because 2,3,4-tri-*O*-Me-Rha was present in *M. smegmatis* mc²155 but was not identified in *M. avium* species (8, 25).

When the *gtf2* gene was disrupted, we detected 6-d-Tal without Rha derivatives in GC/MS analysis, which demonstrates that the *gtf2* gene contributes to the transfer of Rha to the fatty acyl-tetrapeptide core (Fig. 3C). In addition, complementation revealed that the *gtfB* gene of *M. avium* had the same function as *gtf2* (Fig. 8). In the previous studies of GPL biosyntheses, the mutant accumulating 6-d-Tal-containing derivatives without the Rha residue have not been isolated from GPL-producing species so far. Our results directly indicated for the first time that 6-d-Tal-containing derivatives could be an intermediate for the biosynthetic pathways of GPLs.

As for the order of glycosylation steps regulated by *gtf1* and *gtf2*, we cannot determine which step takes place earlier, since both disruptants accumulated the intermediates having different component (Fig. 3B and C). For *M. avium* serovar 2, Eckstein et al. proposed a pathway in which the transfer of the Rha residue to the fatty acyl-tetrapeptide core occurred prior to that of 6-d-Tal, because a mutant strain, 104Rg, having the *gtfA* region deleted, accumulated the fatty acyl-tetrapeptide core with only the Rha residue (13). However, our results lead to the interesting possibility that there are two alternative glycosylation pathways for the formation of nsGPLs (Fig. 9). If the glycosylation should occur in a single pathway, we would expect the accumulation of a nonglycosylated intermediate in either of the disruptants, because one of the genes, *gtf1* or *gtf2*, would be responsible for the first step of glycosylation converting the fatty acyl-tetrapeptide core to a glycosylated intermediate. Thus, the detection of glycosylated intermediates from both Δgtf1 and Δgtf2 suggests that (i) the fatty acyl-tetrapeptide core could be the substrate for both Gtf1 and Gtf2 and (ii) the glycosylated intermediates could also be the substrates for both Gtf1 and Gtf2. We prove here that Gtf1 and Gtf2 have broad substrate specificity and propose that the fatty acyl-tetrapeptide core is glycosylated by Gtf1 and Gtf2 at the same

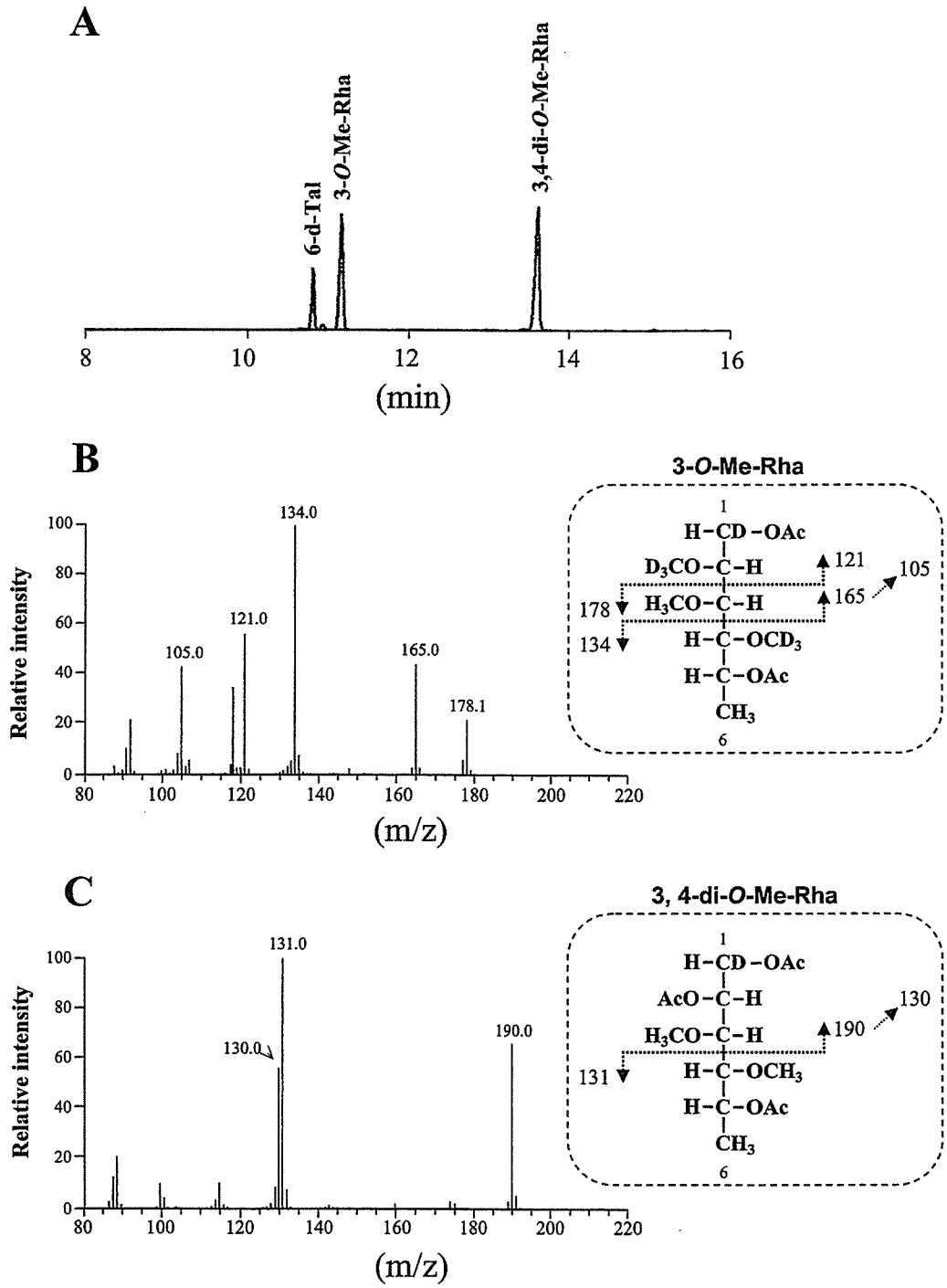

FIG. 5. GC/MS analysis of alditol acetates of sugars released from perdeuteriomethylated GPL-5. (A) GC profile. (B) Mass spectrum and fragment ion assignment corresponding to 3-*O*-Me-Rha. (C) Mass spectrum of fragment ion assignment corresponding to 3,4-di-*O*-Me-Rha.

time and then converted to the nsGPLs having both 6-d-Tal and *O*-Me-Rha via cross-glycosylations (Fig. 9).

Structural determination of GPL-5 and GPL-6 revealed that L-alaninol of the fatty acyl-tetrapeptide core was glycosylated with disaccharide (3-*O*-Me- and 3,4-di-*O*-Me-Rha), which was structurally different from GPLs including GPL-1 to -4 and ssGPLs (Fig. 6). However, it is reported that *M. fortuitum* complex produced GPLs which are glycosylated as in GPL-5 and GPL-6 as major components (19, 20). Therefore, these observations suggest that this type of glycosylation is not specific for *M. smegmatis*. GC/MS analyses of GPL-5 and GPL-6 indicated the presence of 3-*O*-Me-Rha in addition to 3,4-di-*O*-Me-Rha, and analyses of perdeuteriomethylated GPL-5 and GPL-6 showed that position C-1 of 3-*O*-Me-Rha is linked to position C-2 of 3,4-di-*O*-Me-Rha. Recent studies have shown that *M. smegmatis* mc^2155 newly produces two polar GPLs

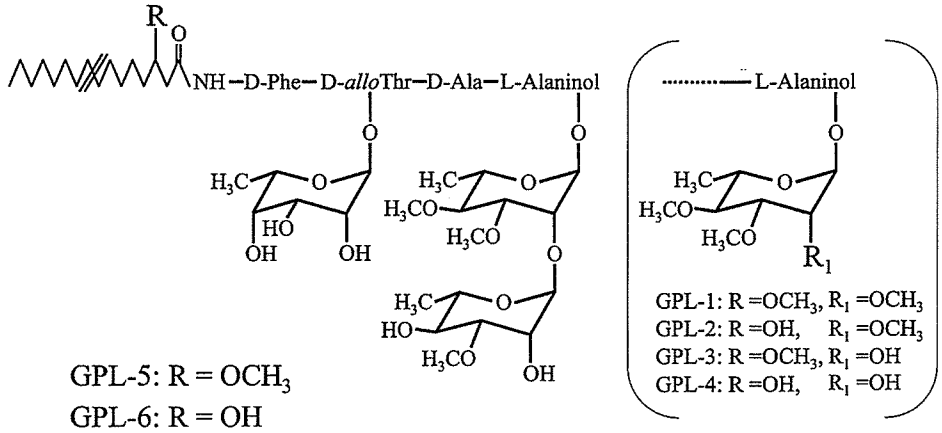

FIG. 6. Proposed structures of GPL-5 and GPL-6. Figure in parentheses shows the structure of GPL-1, GPL-2, GPL-3, and GPL-4, which were characterized in previous studies (10, 16, 25).

which contained two units of 3,4-di-*O*-Me-Rha at L-alaninol of the fatty acyl-tetrapeptide core with no 3-*O*-Me-Rha at any other position when cultured in carbon-limited medium (23, 24). However, the reason for not being able to detect 3-*O*-Me-Rha remains unknown.

In the *gtf3*-overexpressed strain Wt/pMVgtf3, the productivities of GPL-5 and GPL-6 were much higher than those of other GPLs (Fig. 7). So, we can speculate that the expression level of *gtf3* is usually repressed and could be regulated by some environmental factors, such as the nutrient condition or the gene encoding sigma factor (23, 24). GC/MS analyses showed that GPL-5 and GPL-6 have the structures in which 3-*O*-Me-Rha is linked to GPL-3 and GPL-4. These results suggest that GPL-3 and GPL-4 could be the precursors of GPL-5 and GPL-6, respectively, and in Wt/pMVgtf3, overexpression of *gtf3* resulted in 2-*O*-rhamnosylation of 3,4-di-*O*-Me-Rha in GPL-3 and GPL-4 instead of 2-*O*-methylation for converting to GPL-1 and GPL-2, so that GPL-5 and GPL-6 were synthesized.

Figure 9 represents proposed glycosylation steps related to *M. smegmatis* and *M. avium*. We showed that the functions of *gtf1* and *gtf2* corresponded to those of *gtfA* and *gtfB*, respectively. This finding demonstrates that the biosynthetic pathway for nsGPLs, which is the glycosylation of the fatty acyl-tetrapeptide core with the 6-d-Tal and Rha residues, is common between *M. smegmatis* and *M. avium*. Moreover, the biochemical characterization of Δgtf2 and Δgtf1 suggested that the glycosylation pathways for nsGPLs might not be stringent. On the other hand, it has been shown that the *rtfA* gene of *M. avium* triggers the biosynthesis of ssGPLs by transfer of Rha to 6-d-Tal of nsGPLs (12). In *M. smegmatis*, our results indicated that the *gtf3* gene plays a role in synthesis of 3-*O*-Me-rhamno-

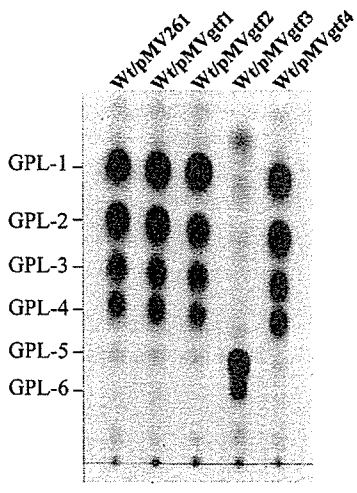

FIG. 7. TLC analyses of crude GPL extracts from the *M. smegmatis* mc^{2}155 strain (Wt) transformed with *gtf* expression vectors. Total lipid fraction after mild alkaline hydrolysis was spotted on plates and developed in $CHCl_3$-CH_3OH (9:1 [vol/vol]). GPLs were visualized by spraying with 10% H_2SO_4 and charring. Each total lipid fraction was extracted from an equal weight of harvested cells.

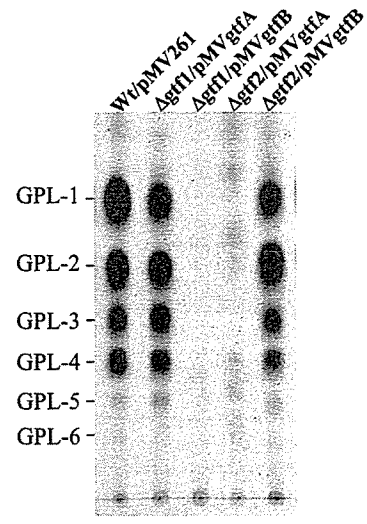

FIG. 8. TLC analyses of crude GPL extracts from the *M. smegmatis* mc^{2}155 strain (Wt) and its gene disruptants transformed with *M. avium* *gtfA* and *gtfB*. Total lipid fraction after mild alkaline hydrolysis was spotted on plates and developed in $CHCl_3$-CH_3OH (9:1 [vol/vol]). GPLs were visualized by spraying with 10% H_2SO_4 and charring. Each total lipid fraction was extracted from an equal weight of harvested cells.

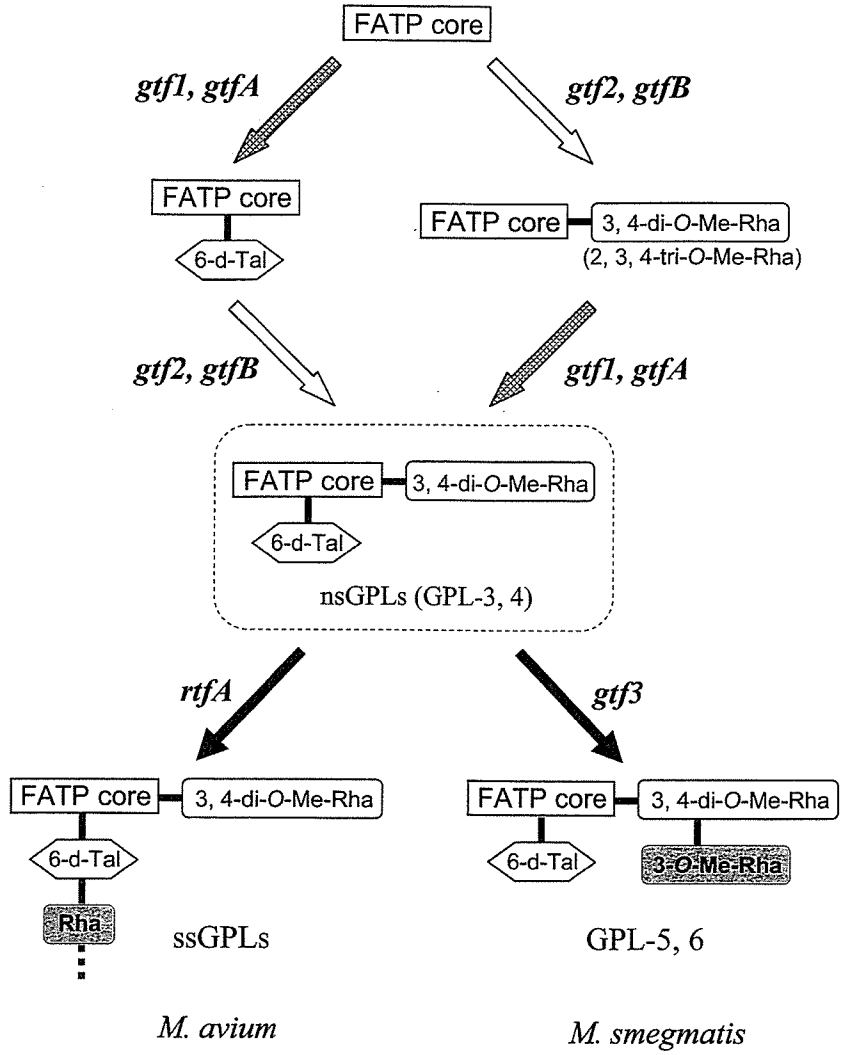

FIG. 9. Proposed biosynthetic pathways for GPLs of *M. smegmatis* and *M. avium*. FATP core, fatty acyl-tetrapeptide core.

syl-(1→2)-3,4-di-*O*-Me-Rha linked to L-alaninol of the fatty acyl-tetrapeptide core by transfer of an extra Rha residue to nsGPLs. Thus, the *rtfA* and *gtf3* genes have the ability to confer the biosynthetic differences between *M. avium* and *M. smegmatis*, suggesting that these genes may be responsible for the phylogenetic distinctions in the two species of mycobacteria.

ACKNOWLEDGMENTS

We thank W. R. Jacobs, Jr. (Albert Einstein College of Medicine, N.Y.), for providing us with the specialized transducing phage system.

This work was supported in part by grants from Health Science Research Grants—Research on Emerging and Re-emerging Infectious Diseases, Grant-in-Aid for Research on HIV/AIDS, the Ministry of Health, Labor and Welfare, Japan.

REFERENCES

1. **Aspinall, G. O., D. Chatterjee, and P. J. Brennan.** 1995. The variable surface glycolipids of mycobacteria: structures, synthesis of epitopes, and biological properties. Adv. Carbohydr. Chem. Biochem. **51:**169–242.
2. **Bardarov, S., S. Bardarov, Jr., M. S. Pavelka, Jr., V. Sambandamurthy, M. Larsen, J. Tufariello, J. Chan, G. Hatfull, and W. R. Jacobs, Jr.** 2002. Specialized transduction: an efficient method for generating marked and unmarked targeted gene disruptions in *Mycobacterium tuberculosis*, *M. bovis* BCG, and *M. smegmatis*. Microbiology **148:**3007–3017.
3. **Barrow, W. W., T. L. Davis, E. L. Wright, V. Labrousse, M. Bachelet, and N. Rastogi.** 1995. Immunomodulatory spectrum of lipids associated with *Mycobacterium avium* serovar 8. Infect. Immun. **63:**126–133.
4. **Belisle, J. T., K. Klaczkiewicz, P. J. Brennan, W. R. Jacobs, Jr., and J. M. Inamine.** 1993. Rough morphological variants of *Mycobacterium avium*. Characterization of genomic deletions resulting in the loss of glycopeptidolipid expression. J. Biol. Chem. **268:**10517–10523.
5. **Billman-Jacobe, H., M. J. McConville, R. E. Haites, S. Kovacevic, and R. L. Coppel.** 1999. Identification of a peptide synthetase involved in the biosynthesis of glycopeptidolipids of *Mycobacterium smegmatis*. Mol. Microbiol. **33:**1244–1253.
6. **Bjorndal, H., C. G. Hellerqvist, B. Lindberg, and S. Svensson.** 1970. Gas-liquid chromatography and mass spectrometry in methylation analysis of polysaccharides. Angew. Chem. Int. Ed. **9:**610–619.
7. **Brennan, P. J., and H. Nikaido.** 1995. The envelope of mycobacteria. Annu. Rev. Biochem. **64:**29–63.
8. **Chatterjee, D., and K. H. Khoo.** 2001. The surface glycopeptidolipids of mycobacteria: structures and biological properties. Cell. Mol. Life Sci. **58:** 2018–2042.
9. **Ciucanu, I., and F. Kerek.** 1984. A simple and rapid method for the permethylation of carbohydrates. Carbohydr. Res. **131:**209–217.
10. **Daffe, M., M. A. Laneelle, and G. Puzo.** 1983. Structural elucidation by field desorption and electron-impact mass spectrometry of the C-mycosides isolated from *Mycobacterium smegmatis*. Biochim. Biophys. Acta **751:**439–443.
11. **Daffe, M., and P. Draper.** 1998. The envelope layers of mycobacteria with reference to their pathogenicity. Adv. Microb. Physiol. **39:**131–203.
12. **Eckstein, T. M., F. S. Silbaq, D. Chatterjee, N. J. Kelly, P. J. Brennan, and J. T. Belisle.** 1998. Identification and recombinant expression of a *Mycobac-*

terium avium rhamnosyltransferase gene (*rtfA*) involved in glycopeptidolipid biosynthesis. J. Bacteriol. **180:**5567–5573.

13. **Eckstein, T. M., J. T. Belisle, and J. M. Inamine.** 2003. Proposed pathway for the biosynthesis of serovar-specific glycopeptidolipids in *Mycobacterium avium* serovar 2. Microbiology **149:**2797–2807.
14. **Etienne, G., C. Villeneuve, H. Billman-Jacobe, C. Astarie-Dequeker, M. A. Dupont, and M. Daffe.** 2002. The impact of the absence of glycopeptidolipids on the ultrastructure, cell surface and cell wall properties, and phagocytosis of *Mycobacterium smegmatis*. Microbiology **148:**3089–3100.
15. **Horgen, L., E. L. Barrow, W. W. Barrow, and N. Rastogi.** 2000. Exposure of human peripheral blood mononuclear cells to total lipids and serovar-specific glycopeptidolipids from *Mycobacterium avium* serovars 4 and 8 results in inhibition of TH1-type responses. Microb. Pathog. **29:**9–16.
16. **Jeevarajah, D., J. H. Patterson, M. J. McConville, and H. Billman-Jacobe.** 2002. Modification of glycopeptidolipids by an *O*-methyltransferase of *Mycobacterium smegmatis*. Microbiology **148:**3079–3087.
17. **Kano, H., T. Doi, Y. Fujita, H. Takimoto, I. Yano, and Y. Kumazawa.** 2005. Serotype-specific modulation of human monocyte functions by glycopeptidolipid (GPL) isolated from *Mycobacterium avium* complex. Biol. Pharm. Bull. **28:**335–339.
18. **Krzywinska, E., S. Bhatnagar, L. Sweet, D. Chatterjee, and J. S. Schorey.** 2005. *Mycobacterium avium* 104 deleted of the methyltransferase D gene by allelic replacement lacks serotype-specific glycopeptidolipids and shows attenuated virulence in mice. Mol. Microbiol. **56:**1262–1273.
19. **Lopez Marin, L. M., M. A. Laneelle, D. Prome, M. Daffe, G. Laneelle, and J. C. Prome.** 1991. Glycopeptidolipids from *Mycobacterium fortuitum*: a variant in the structure of C-mycoside. Biochemistry **30:**10536–10542.
20. **Lopez-Marin, L. M., N. Gautier, M. A. Laneelle, G. Silve, and M. Daffe.** 1994. Structures of the glycopeptidolipid antigens of *Mycobacterium abscessus* and *Mycobacterium chelonae* and possible chemical basis of the serological cross-reactions in the *Mycobacterium fortuitum* complex. Microbiology **140:**1109–1118.
21. **Minami, H.** 1998. Promotion of phagocytosis and prevention of phagosome-lysosome (P-L) fusion in human peripheral blood monocytes by serotype specific glycopeptidolipid (GPL) antigen of *Mycobacterium avium* complex (MAC). Kekkaku **73:**545–556.
22. **Miyamoto, Y., T. Mukai, F. Takeshita, N. Nakata, Y. Maeda, M. Kai, and M. Makino.** 2004. Aggregation of mycobacteria caused by disruption of fibronectin-attachment protein-encoding gene. FEMS Microbiol. Lett. **236:** 227–234.
23. **Mukherjee, R., M. Gomez, N. Jayaraman, I. Smith, and D. Chatterji.** 2005. Hyperglycosylation of glycopeptidolipid of *Mycobacterium smegmatis* under nutrient starvation: structural studies. Microbiology **151:**2385–2392.
24. **Ojha, A. K., S. Varma, and D. Chatterji.** 2002. Synthesis of an unusual polar glycopeptidolipid in glucose-limited culture of *Mycobacterium smegmatis*. Microbiology **148:**3039–3048.
25. **Patterson, J. H., M. J. McConville, R. E. Haites, R. L. Coppel, and H. Billman-Jacobe.** 2000. Identification of a methyltransferase from *Mycobacterium smegmatis* involved in glycopeptidolipid synthesis. J. Biol. Chem. **275:**24900–24906.
26. **Recht, J., and R. Kolter.** 2001. Glycopeptidolipid acetylation affects sliding motility and biofilm formation in *Mycobacterium smegmatis*. J. Bacteriol. **183:**5718–5724.
27. **Snapper, S. B., R. E. Melton, S. Mustafa, T. Kieser, and W. R. Jacobs, Jr.** 1990. Isolation and characterization of efficient plasmid transformation mutants of *Mycobacterium smegmatis*. Mol. Microbiol. **4:**1911–1919.
28. **Stover, C. K., V. F. de la Cruz, T. R. Fuerst, J. E. Burlein, L. A. Benson, L. T. Bennett, G. P. Bansal, J. F. Young, M. H. Lee, G. F. Hatfull, S. B. Snapper, R. G. Barletta, W. R. Jacobs, Jr., and B. R. Bloom.** 1991. New use of BCG for recombinant vaccines. Nature **351:**456–460.
29. **Tassell, S. K., M. Pourshafie, E. L. Wright, M. G. Richmond, and W. W. Barrow.** 1992. Modified lymphocyte response to mitogens induced by the lipopeptide fragment derived from *Mycobacterium avium* serovar-specific glycopeptidolipids. Infect. Immun. **60:**706–711.
30. **Torrelles, J. B., D. Ellis, T. Osborne, A. Hoefer, I. M. Orme, D. Chatterjee, P. J. Brennan, and A. M. Cooper.** 2002. Characterization of virulence, colony morphotype and the glycopeptidolipid of *Mycobacterium avium* strain 104. Tuberculosis (Edinburgh) **82:**293–300.
31. **Vergne, I., and M. Daffe.** 1998. Interaction of mycobacterial glycolipids with host cells. Front. Biosci. **3:**d865–d876.
32. **Villeneuve, C., G. Etienne, V. Abadie, H. Montrozier, C. Bordier, F. Laval, M. Daffe, I. Maridonneau-Parini, and C. Astarie-Dequeker.** 2003. Surface-exposed glycopeptidolipids of *Mycobacterium smegmatis* specifically inhibit the phagocytosis of mycobacteria by human macrophages. Identification of a novel family of glycopeptidolipids. J. Biol. Chem. **278:**51291–51300.

Identification of *Mycobacterium* species by comparative analysis of the *dnaA* gene

Tetsu Mukai, Yuji Miyamoto, Toshio Yamazaki & Masahiko Makino

Department of Microbiology, Leprosy Research Center, National Institute of Infectious Diseases (NIID), Higashimurayama, Tokyo, Japan

Correspondence: Tetsu Mukai, Department of Microbiology, Leprosy Research Center, National Institute of Infectious Diseases (NIID), 4-2-1, Aobacho, Higashimurayama, Tokyo, 189-0002, Japan. Tel.: +81 42 391 8211; fax: +81 42 391 8807; e-mail: tmukai@nih.go.jp

Received 19 July 2005; revised 5 October 2005; accepted 11 October 2005.
First published online 25 November 2005.

doi:10.1111/j.1574-6968.2005.00031.x

Editor: Roger Buxton

Keywords
Mycobacterium spp.; *dnaA* gene; differential diagnosis; LAMP assay.

Abstract

For the establishment of a diagnostic tool for mycobacterial species, a part of the *dnaA* gene was amplified and sequenced from clinically relevant 27 mycobacterial species as well as 49 clinical isolates. Sequence variability in the amplified segment of the *dnaA* gene allowed the differentiation of all species except for *Mycobacterium tuberculosis, Mycobacterium africanum* and *Mycobacterium microti,* which had identical sequences. Partial sequences of *dnaA* from clinical isolates belonging to three frequently isolated species revealed a very high intraspecies similarity, with a range of 96.0–100%. Based on the *dnaA* sequences, a species-specific primer set for *Mycobacterium kansasii* and *Mycobacterium gastri* was successfully designed for a simple loop-mediated isothermal amplification method. These results demonstrate that the variable sequences in the *dnaA* gene were species specific and were sufficient for the development of an accurate and rapid diagnosis of *Mycobacterium* species.

Introduction

Increasing reports of opportunistic infection by nontuberculous mycobacteria (NTM) in immunocompromised patients such as AIDS patients and elderly people are a matter of serious concern to public health (Horsburg, 1991; Montessori *et al.*, 1996; Primm *et al.*, 2004). The routine diagnosis of mycobacteriosis relies primarily on the detection of acid-fast-stained bacilli in the samples by microscopic observation, and the infecting mycobacterial species can be identified with conventional tests including observation of colony morphology and pigmentation, growth rate, and biochemical characteristics (Cernoch *et al.*, 1994; Metchock *et al.*, 1999). Disadvantages of this approach include the time taken to provide clinically relevant information. The clinician must initiate therapy for *Mycobacterium tuberculosis* against NTM infection several weeks before species identification (Montessori *et al.*, 1996), which may increase health care costs, and may reduce the social activity of the patients. Therefore rapid detection and identification of the species level of mycobacteria is required, both to decide whether measures are needed to prevent the spread of the disease and for adequate therapy (American Thoracic Society, 1997).

The mycobacterium species often implicated in NTM infection are *Mycobacterium avium–Mycobacterium intracellulare* complex (MAC), *Mycobacterium kansasii, Mycobacterium chelonae, Mycobacterium abscessus,* and *Mycobacterium xenopi* (Wayne & Sramek, 1992; Metchock *et al.*, 1999; Primm *et al.*, 2004). *Mycobacterium gordonae, Mycobacterium gastri,* or most of the rapidly growing species are rarely pathogenic, but are often encountered as contaminant in clinical samples. Therefore, the discrimination of these species from pathogenic ones is an important diagnostic issue (Primm *et al.*, 2004).

Several studies have been conducted to develop rapid methods based on molecular technique for identifying mycobacterial species in recent years. The DNA sequences reported for such usage are those of 16S rRNA gene (Kirschner *et al.*, 1993; De Beenhouwer *et al.*, 1995; Cloud *et al.*, 2002), *recA* (Blackwood *et al.*, 2000), *rpoB* (Kim *et al.*, 1999), *gyrB* (Kasai *et al.*, 2000), *hsp65* (Plikaytis *et al.*, 1992; Brunello *et al.*, 2001), or 16S–23S internal transcribed spacer (ITS) (De Smet *et al.*, 1995; Roth *et al.*, 1998). The 16S rRNA gene and ITS-based methods are currently widely accepted as rapid and accurate for identifying mycobacteria (Plikaytis *et al.*, 1992; De Smet *et al.*, 1995; Park *et al.*, 2000; Turenne *et al.*, 2001). However, some species have the same sequence or a very high similarity (Kim *et al.*, 1999; Kasai *et al.*, 2000). This fact indicates the need to develop more reliable and user-friendly molecule-based diagnostic tools.

Recently, Notomi *et al.* (2000) have reported a novel nucleic acid amplification method, termed loop-mediated

isothermal amplification (LAMP), that amplifies DNA with high specificity, efficacy, and rapidity under isothermal conditions. The LAMP reaction requires a *Bst* DNA polymerase with strand displacement activity and a set of four specially designed primers that recognize six distinct sequences on the target DNA, the specificity of which should be extremely high. The amplification products are stem-loop DNA structures with several inverted repeats of the target. The advantage of the LAMP method is that the reaction is performed under isothermal conditions of between 60 and 65 °C. As a result, it requires only simple and cost-effective reaction equipment. The LAMP method has emerged as a powerful tool to facilitate genetic testing for various infectious diseases (Enosawa *et al.*, 2003; Iwamoto *et al.*, 2003; Kuboki *et al.*, 2003; Ihira *et al.*, 2004; Parida *et al.*, 2004; Thai *et al.*, 2004).

The purpose of our work is to identify a species-specific region of *Mycobacterium* sp., and to develop a LAMP assay that can differentiate clinically relevant species.

Materials and methods

Bacterial strains and preparation of genomic DNA

The bacteria used in this study comprised 27 strains and 49 clinical isolates as shown in Table 1. All strains except for *Mycobacterium leprae* were cultured on 1% Ogawa medium (Nissui, Tokyo, Japan) at 37 °C. *Mycobacterium leprae* was prepared from infected nude mouse food pad (Shepard, 1960). Genomic DNA was extracted from mycobacterial strains as follows. Mycobacterial cells were resuspended in 1.8 mL of sterile phosphate-buffered saline (PBS) containing 0.1 mm diameter zirconia/silica beads (BioSpec Products Inc., Bartlesville, OK). The mixture was beaded for 20 s with a Beads Homogenizer Model BC-20 (Central Scientific Commerce, Tokyo, Japan), transferred to a 1.5 mL microcentrifuge tube, and the genomic DNA was purified with proteinase K treatment and phenol/chloroform extraction followed by ethanol precipitation, then suspended in 100 μL distilled water.

Table 1. *Mycobacterium* species and strains used in this study and results of the loop-mediated isothermal amplification assay

			Primer set	
Species	Strains	Accession number	Kan32	Gas583
Mycobacterium abscessus	JATA 63-01 (ATCC 19977)	AB087684	–	–
Mycobacterium africanum	KK 13-02 (ATCC 25420)	AB087685	–	–
Mycobacterium avium	JATA 51-01 (ATCC 25291)	AB087686	–	–
	Clinical isolate 22 strains			
Mycobacterium bovis	JATA 12-01 (ATCC 19210)	AB087687	–	–
Mycobacterium chelonae	JATA 62-01 (ATCC 35752)	AB087688	–	–
Mycobacterium fortuitum	JATA 61-01 (ATCC 6841)	AB087689	–	–
Mycobacterium gastri	KK 44-02 (ATCC 15754)	AB087690	–	+
Mycobacterium gordonae	JATA 33-01 (ATCC 14470)	AB087691	–	–
Mycobacterium intracellulare	JATA 52-01 (ATCC 13950)	AB087692	–	–
	Clinical isolate 17 strains			
Mycobacterium kansasii	KK 21-01 (ATCC 12478)	AB087693	+	–
	Clinical isolate 10 strains		+	–
Mycobacterium leprae	Thai-53	AB087694	–	–
Mycobacterium malmoense	JATA 47-01 (ATCC 29571)	AB087695	–	–
Mycobacterium marinum	JATA 22-01 (ATCC 927)	AB087696	–	–
Mycobacterium microti	KK 14-01 (ATCC 19422)	AB087697	–	–
Mycobacterium nonchromogenicum	JATA 45-01 (ATCC 19530)	AB087698	–	–
Mycobacterium parafortuitum	ATCC 25807	AB087699	–	–
Mycobacterium phlei	ATCC 19249	AB087700	–	–
Mycobacterium scrofulaceum	JATA 31-01 (ATCC 19981)	AB087701	–	–
Mycobacterium simiae	KK 23-08 (ATCC 25275)	AB087702	–	–
Mycobacterium smegmatis	JATA 64-01	AB087703	–	–
Mycobacterium szulgai	JATA 32-01	AB087704	–	–
Mycobacterium terrae	KK 46-01 (ATCC 15755)	AB087705	–	–
Mycobacterium triviale	KK 50-02 (ATCC 23292)	AB087706	–	–
Mycobacterium tuberculosis	JATA 11-01 (H37Rv)	AB087707	–	–
Mycobacterium ulcerans	KK 43-01	AB087708	–	–
Mycobacterium vaccae	KK 66-01	AB087709	–	–
Mycobacterium xenopi	KK 42-01 (ATCC 19250)	AB087710	–	–

All strains were kindly donated by Dr Kashiwabara, NIID.

Clinical isolates were identified by Amplicore *Mycobacterium* kit (Roche Pharma, Basel, Switzerland) or conventional biochemical test (Jamal *et al.*, 2000).

Amplification of the region within *dnaA* gene

Highly polymorphic regions flanked by conserved regions were identified by aligning the *Mycobacterium* spp. *dnaA* sequences, which were available in GenBank at the time this study was initiated. These regions were used to design a pair of degenerate primers, U1F 5′-GTS CAR AAC GAR ATC GAR CG-3′ and U1R 5′-CCB GAY TCR CCC CAG ATG AA-3′. A schematic representation of the primer design is shown in Fig. 1a. PCR was performed in a TAKARA Thermal Cycler MP (TAKARA Biomedical, Otsu, Japan) with a reaction mixture consisting of 1 μL of genomic DNA, each deoxynucleoside triphosphate at a concentration of 200 μM, each primer at a concentration of 0.4 μM, 1 × PCR buffer with 1.5 mM $MgCl_2$ (TAKARA Biomedical), and 1.25 U of ExTaq (TAKARA Biomedical), with 10 μL PCRX Enhancer System solution (Gibco BRL, Rockville, MD) in a total volume of 50 μL. The PCR thermocycles were 3 min at 94 °C, followed by 30 cycles of 94 °C for 10 s, 50 °C for 20 s, and 72 °C for 45 s, with a final extension step at 72 °C for 7 min. PCR products were visualized by UV illumination of an ethidium bromide-stained 1.5% agarose gel and cut out to purify with EASYTRAP Ver.2 (TAKARA Biomedical) according to the manufacturer's instruction.

DNA sequencing and sequencing analysis

The ABI Prism BigDye Terminator v3.1 Cycle Sequencing Kit (PE Biosystems, Foster City, CA) was used for the sequencing of the PCR products. The same primers for amplification were used for sequencing. The sequencing reaction was performed in accordance with the instruction of the manufacturer. Sequencing products were purified with a Centrisep column (Princeton Separations, Adelphia, NJ).

The sequencing output was analyzed by using the DNA Sequence Analyzer computer software (PE Biosystems). The partial *dnaA* sequences were aligned using the Clustal W algorithm (Thompson *et al.*, 1994) of the software DNASpace ver. 3.5 (Hitachi Software Engineering, Yokohama, Japan), and the alignment was manually corrected. A phylogenetic tree was generated by DNASpace ver. 3.5 (Hitachi Software Engineering) with a total of 1000 bootstraps. Pairwise similarity of the partial *dnaA* sequences was determined by using DNASIS package (Hitachi Software Engineering).

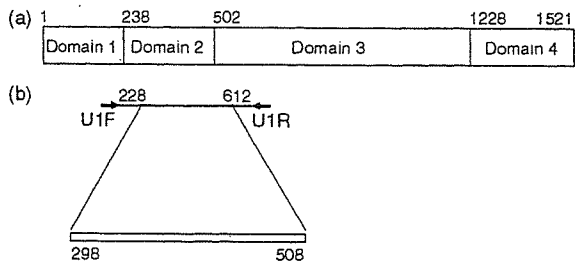

Fig. 1. Schematic representation of the DnaA protein and primer design for the amplification of the partial mycobacterial *dnaA* gene. Number indicates the nucleotide position of *Mycobacterium tuberculosis*, GenBank accession number AL021427. (a) The DnaA protein from *M. tuberculosis* contains four domains. Domain 1 is involved in interaction with DnaB. Domain 2 constitutes a flexible loop. DNA unwinding required Domain 3. Domain 4 is sufficient for specific binding to DNA. Primers U1F and U1R were used to generate about 400 bp fragment from *dnaA* of 27 mycobacterial spp. (b) Analysis and comparison region used in this study are indicated by a bar (298–508 bp).

Species-specific LAMP assay for *Mycobacterium kansasii* and *Mycobacterium gastri*

A set of four primers comprising two inner primers and two outer primers that recognized six distinct regions on the target sequence were designed with PrimerExplorer Ver.3 (Fujitu, Tokyo, Japan). The detailed sequences of the primers are shown in Fig. 3. The two inner primers are called the forward inner primer (FIP) and the backward inner primer (BIP), and each contains two distinct sequences corresponding to the sense and antisense sequences of the target DNA, one for priming in the first stage and the other for self-priming in late stages. FIP contains the sequence complementary F1 (F1c) and F2. BIP contains the complementary B1 (B1c) and B2. The two outer primers consist of F3 and B3.

The LAMP reaction was carried out in 25 μL of reaction mixture by using the Loopamp DNA amplification kit (Eiken Chemical Co. Ltd., Tochigi, Japan) containing 2.4 μM (each) FIP and BIP, 0.2 μM (each) of the outer primers, F3 and B3, 20 mM Tris-HCl (pH 8.8), 10 mM KCl, 8 mM $MgSO_4$, 10 mM $(NH_4)_2SO_4$, 0.1% Tween 20, 0.8 M betaine, 1.4 mM (each) of dNTP, 8 U of *Bst* DNA polymerase (New England BioLabs, Beverly, MA), and the template DNA. Amplification was undertaken in 0.5 μL microtubes in a heatblock under isothermal conditions of 63 °C for 60 min, followed by 80 °C for 2 min to terminate the reaction. Positive and negative controls were included in each run, and precautions to prevent cross-contamination were observed. Two microliter aliquots of LAMP products were subjected to electrophoresis on a 4% agarose gel in Tris-borate-EDTA buffer followed by staining with ethidium bromide and were visualized on a UV transilluminator at 302 nm. The specificity of the LAMP-amplified products were further validated by restriction enzyme digestion with *Nae*I and *Hae*II for *M. kansasii* and *M. gastri*, respectively. The diluted genomic DNA was used for determining the sensitivity of the species-specific LAMP assay.

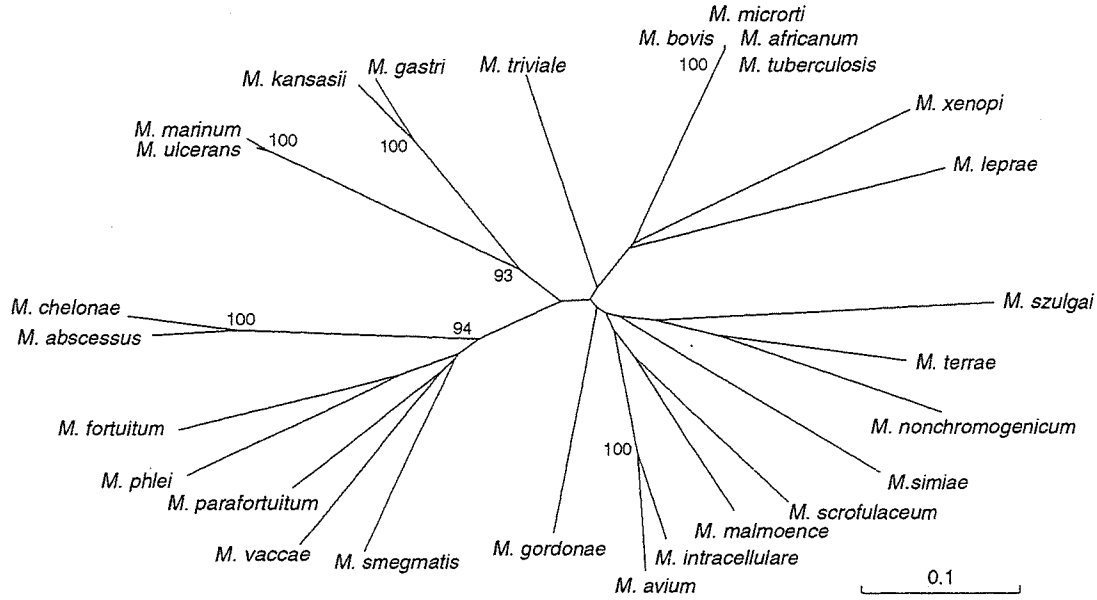

Fig. 2. Phylogenetic relationship of 27 *Mycobacterium* species. Unrooted tree based on the *dnaA* sequences. The tree was generated from DNASpace (Hitachi Software Engineering) with the Clustal W algorithm. The numbers on the dendrogram indicate the percentages of occurrence in 1000 bootstrapped trees; only values of > 90% are shown.

Results

Comparison of partial *dnaA* sequence to identify the *Mycobacterium* species

For the species identification of mycobacterial species, we analyzed some possible variable regions of mycobacterial sequences deposited in the GenBank, and found the 5′ part of the *dnaA* gene as a candidate target for PCR amplification. The PCR products with U1F and U1R, from 27 mycobacterial species, showed the ragged pattern around 400 bp in size (data not shown). Therefore, we determined nucleotide sequences, corresponding to position 228–612 bp of *Mycobacterium tuberculosis*, of all 27 species (Fig. 1a). The alignment of the sequence shows that the region (298–508 bp) in the amplified products had the highest species-specific variability (Fig. 1b). The size of the variable fragment in *dnaA* ranged from 154 bp in *M. triviale* to 232 bp in *M. kansasii*. The variable region exhibits a reasonable number of nucleotide substitution and insertion or deletion sites, which is important for the development of a differential diagnostic tool. The lowest interspecies similarity was 28.2% in *M. leprae* versus *M. vaccae*. The similarity between *M. avium* and *M. intracellulare* was 78.3% and that between *M. marinum* and *M. ulcerans* was 97.7%. Pathogenic *M. kansasii* were easily differentiated from nonpathogenic *M. gastri* (83.6%). The sequences of *M. tuberculosis*, *M. microti*, *M. africanum*, and *M. bovis* were found to be identical, except for one nucleotide substitution that occurred in *M. bovis*. When clinical isolates from clinically relevant mycobacterial strains were analyzed, the following minor variation was found among each species: 97.7–100% (*M. avium*) and 96.0–100% (*M. intracellulare*). We did not find any intraspecies variation in 10 clinical isolates and the standard strain of *M. kansasii*. Because other reports using different systems revealed the existence of more than one sequevar (Yang *et al.*, 1993; Alcaide *et al.*, 1997), we may need to examine a bigger number of clinical isolates.

The unrooted phylogenetic tree showed that the 27 mycobacterial species were resolved by the variable region in the *dnaA* sequence (Fig. 2). All rapidly growing species, *M. abscessus*, *M. chelonae*, *M. fortuitum*, *M. parafortuitum*, *M. phlei*, *M. vaccae*, and *M. smegmatis*, made a cluster that was clearly separated from those of the other species so far examined. On the other hand, *M. kansasii*, *M. gastri*, *M. avium*, and *M. intracellulare* are clinically relevant species; however, the branch of the former two species was obviously segregated from one of the later two species, which was supported by high bootstrap values. The results indicated that the partial *dnaA* sequence could be useful for the differentiation of NTM (Fig. 2).

Identification of mycobacteria by *dnaA* sequence-targeted species-specific LAMP assay

Several sets of primers designed from the *dnaA* sequence were evaluated for their specificity and sensitivity by the LAMP method. One set of primers named Kan-32 for *M. kansasii* and Gas-583 for *M. gastri* was selected (Fig. 3), and

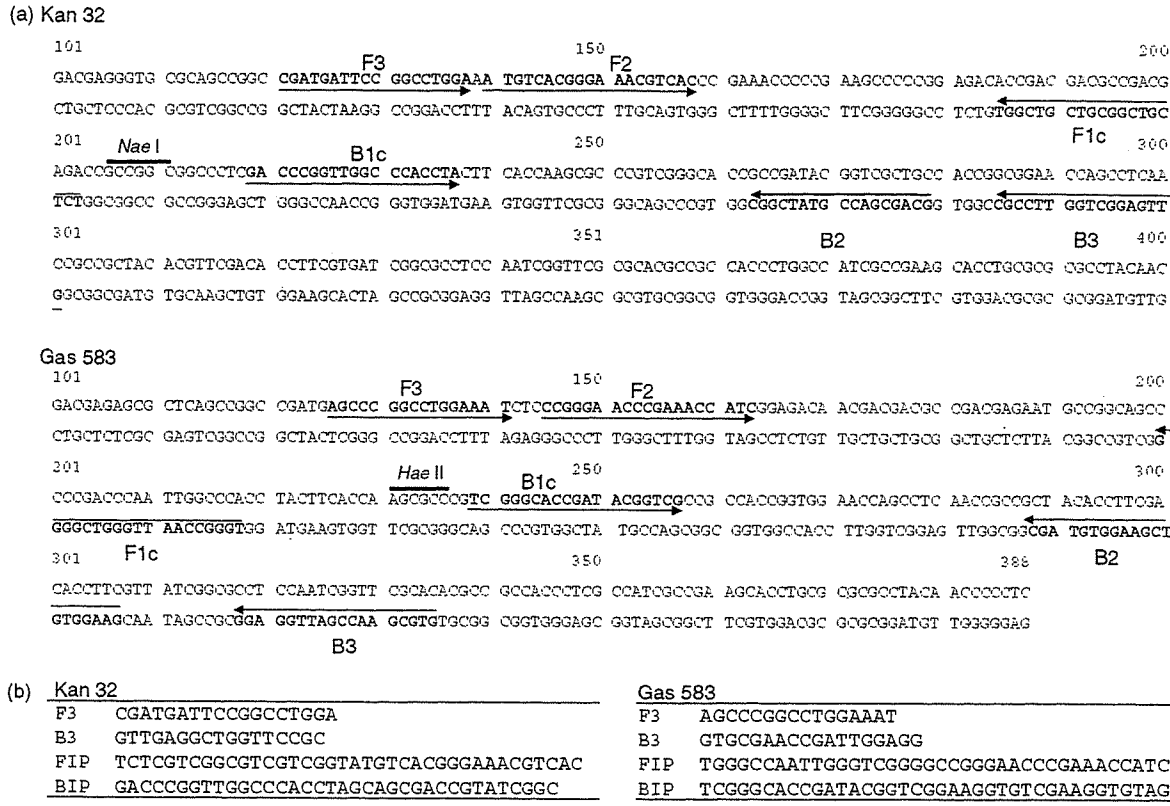

Fig. 3. Location of oligonucleotide primer sets Kan 32 and Gas 583, used for the loop-mediated isothermal amplification method. For *Mycobacterium kansasii* partial *dnaA* gene (GenBank accession number AB087693) and for *Mycobacterium gastri* partial *dnaA* gene (GenBank accession number AB087690). A right arrow indicates the sense sequence which is used as the primer. A left arrow indicates that a complementary sequence is used as the primer. The unique restriction enzyme recognition sites in the amplified product are shown with a bold bar. (b) List of each primer sequence.

by using these primer sets, a successful LAMP product appeared as a ladder of multiple bands (Fig. 3a).

The species specificity and intraspecies stability of each primer set were examined with purified DNA from 27 mycobacterial species and 10 clinical isolates of *M. kansasii*. We subjected each sample to amplification using Kan-32 or Gas-583 primer set. The results obtained by electrophoretic examination are summarized in Table 1. Although 200 pg of nontargeted species DNA were not amplified, significant amplification of targeted respective isolates was observed after a 60 min incubation at 63 °C. To confirm that the amplification products had corresponding DNA structures, the amplified products were digested with restriction enzymes and the size of the fragments was analyzed by electrophoresis. *Nae*I cuts between F1 and B1c for the *M. kansasii* amplicon; *Hae*II was used for the *M. gastri* amplicons. The sizes of the fragments generated after digestion were in good agreement with sizes predicted theoretically from the expected DNA structure: 100 and 93 bp by *Nae*I digestion, and 123 and 98 bp by *Hae*II digestion (Fig. 4a). Thus, we concluded that each primer set was species specific.

We next assessed the sensitivity of the assay. Serially diluted *M. kansasii* or *M. gastri* genomic DNA was used. The results of a typical experiment are shown in Fig. 4b. Amplified DNA was readily visible when 500 copies of genomic DNA were present in a 60 min incubation assay. The detection limit did not change with a longer incubation period (data not shown).

Discussion and conclusions

For the identification of species, a target gene must be conserved among strains and species. As the DnaA protein is generally conserved among microbial organisms (Mizrahi *et al.*, 2000), this coding region could be used for the target analysis. Four functional domains of the DnaA protein have been defined (Messer *et al.*, 1998). Domain 1 is involved in oligomerization and interaction with DnaB, Domain 2 constitutes a flexible loop, Domain 3 has ATPase function, and Domain 4 is sufficient for specific binding to DNA. The variable region that we identified in the *dnaA* sequence was equivalent to the Domain 2 coding nucleotide sequence

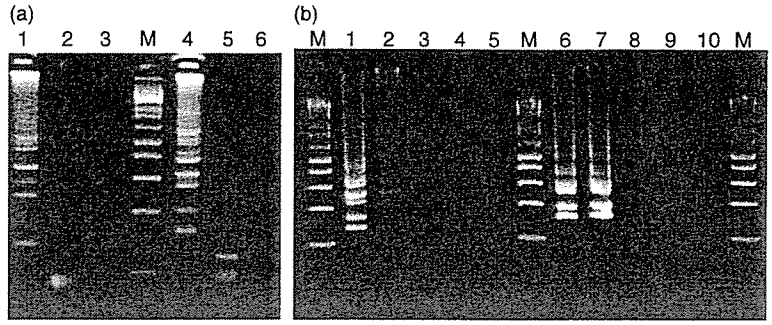

Fig. 4. (a) Four percent agarose gel electrophoresis and restriction enzyme analysis of loop-mediated isothermal amplification (LAMP) products of partial *dnaA* gene of *Mycobacterium kansasii* and *Mycobacterium gastri*. Lanes: M, 100 bp DNA ladder; lanes 1–3, LAMP carried out with *M. kansasii* primer, Kan 32, in the presence of genomic DNA from *M. kansasii* (lanes 1 and 2) and *M. gastri* (lane 3); lane 2, LAMP product from lane 1 after digestion with *Nae* I; lanes 4–6, LAMP carried out with *M. gastri* primer, Gas 583, in the presence of genomic DNA from *M. gastri* (lanes 4 and 5) and *M. kansasii* (lane 6). lane 5, LAMP product from lane 4 after digestion with *Hae* II. (b) Serial dilution of purified *M. kansasii* or *M. gastri* genomic DNA was amplified to determine the sensitivities by LAMP. Lanes: M, 100 bp DNA ladder; lanes 1–5 LAMP carried out with Kan 32 primer set in the presence of genomic DNA of *M. kansasii*, lane 1, 1000 copies; lane 2, 500 copies; lane 3, 100 copies; lane 4, 10 copy; lane 5, distilled water. lanes 6–10 LAMP carried out with gas 583 primer set in the presence of genomic DNA of *M. gastri*, lane 6, 1000 copies; lane 7, 300 copies; lane 8, 100 copies; lanes 9, 10 copy; lane 10, distilled water.

(Fig. 1). This domain is the least conserved region in the *dna A* gene with respect to sequence and length among *M. smegmatis*, *M. tuberculosis*, and *M. leprae* (Fsihi *et al.*, 1996). However, comparative studies of this region using 27 mycobacteria have not been reported and, as far as we know, this is the first report indicating the usefulness of the *dnaA* Domain 2 sequence as a differential diagnostic tool.

An accurate and rapid bacterial identification greatly contributes to this field of medication. Several methods based on molecular biological techniques have been reported. The sequences that have been reported include *hsp65*, 16S rRNA gene, and ITS (Plikaytis *et al.*, 1992; De Smet *et al.*, 1995; Springer *et al.*, 1996; Messer & Weigel, 1997; Roth *et al.*, 1998; Brunello *et al.*, 2001). Each gene has several advantages and disadvantages. An excessive degree of variability is found in the *hsp65* gene (Telenti *et al.*, 1993), which may hinder the development of reliable probes. While 16s rRNA gene sequence is identical in *M. kansasii* and *M. gastri* and shows narrow divergenicity within species (Taylor *et al.*, 1997), ITS sequence can be used to distinguish between *M. kansasii* and *M. gastri* (Roth *et al.*, 1998). While *M. kansasii* is a representative pathogenic mycobacteria, *M. gastri* does not induce an apparent disease. The discrimination between these mycobacteria provides useful information to select the appropriate therapy. The percent similarity of ITS between two species was 93% (Roth *et al.*, 1998), and that of the *dnaA* variable region was found to be 83.6%. These observations may indicate the usefulness of the *dnaA* gene for discrimination of these species, at least in complement with ITS.

The recent trend in genetic testing is to make systems fully automatic with high-throughput analysis. Although this may be an ideal approach, it requires expensive equipment as well as a well-trained person in diagnostic laboratories. The LAMP method could be conducted under isothermal conditions ranging from 60 to 65 °C by a single enzyme. The only equipment needed for LAMP reaction is a regular laboratory water bath or a heat block that furnishes a constant temperature around 63 °C. LAMP does not require a thermal cycling step, and an isothermal reaction for a short time (60 min) is enough to amplify the target DNA to a detectable level. As PCR and other molecular biological techniques are conducted in well-equipped laboratories, these methodologies are often impracticable under a field diagnosis.

In this paper, we demonstrated that the *dnaA* region could be an effective new nucleotide region for the diagnosis of NTM infection and that the LAMP method could be applied for a *dnaA* gene-based differential diagnostic tool.

Acknowledgements

We are grateful to Dr Y. Kashiwabara for the mycobacterial strains. This work was supported in part by a Health Science Research Grants-Research on Emerging and Re-emerging Infectious Diseases, Ministry of Health, Labour and Welfare, Japan.

References

Alcaide F, Richter I, Bernasconi C, Springer B, Hagenau C, Schulze-Robbecke R, Tortoli E, Martin R, Bottger EC & Telenti A (1997) Heterogeneity and clonality among isolates of *Mycobacterium kansasii*: implications for epidemiological and pathogenicity studies. *J Clin Microbiol* **35**: 1959–1964.

American Thoracic Society (1997) Diagnosis and treatment of diseases caused by nontuberculous mycobacteria. *Am J Respir Crit Care Med* **156**: S1–S25.

De Beenhouwer H, Liang Z, De Rijk P, Van Eekeren C & Portaels F (1995) Detection and identification of mycobacteria by DNA amplification and oligonucleotide-specific capture plate hybridization. *J Clin Microbiol* **33**: 2994–2998.

Blackwood KS, He C, Gunton J, Turenne CY, Wolfe J & Kabani AM (2000) Evaluation of *recA* sequences for identification of *Mycobacterium* species. *J Clin Microbiol* **38**: 2846–2852.

Brunello F, Ligozzi M, Cristelli E, Bnora S, Tortoli E & Fontana R (2001) Identification of 54 mycobacterial species by PCR-restriction fragment length polymorphism analysis of the *hsp65* gene. *J Clin Microbiol* **39**: 2799–2806.

Cernoch PL, Enns RK, Saubolle MA & Wallace RA Jr (1994) Laboratory diagnosis of the Mycobacterioses. Cumitech 16A (Weissfield AS, Coordinating ed.), American Society for Microbiology, Washington, DC.

Cloud JL, Neal H, Rosenberry R, Turenne CY, Jama M, Hillyard DR & Carroll1 KC (2002) Identification of *Mycobacterium* spp. by using a commercial 16S ribosomal DNA sequencing kit and additional sequencing libraries. *J Clin Microbiol* **40**: 400–406.

De Smet KA, Brown IN, Yates M & Ivanyi J (1995) Ribosomal internal transcribed spacer sequences are identical among *Mycobacterium avium–intracellulare* complex isolates from AIDS patients, but vary among isolates from elderly pulmonary disease patients. *Microbiology* **141**: 2739–2747.

Enosawa M, Kageyama S, Sawai K, Watanabe K, Notomi T, Onoe S, Mori Y & Yokomizo Y (2003) Use of loop-mediated isothermal amplification of the IS900 sequence for rapid detection of cultured *Mycobacterium avium* subsp. *paratuberculosis*. *J Clin Microbiol* **41**: 4359–4365.

Fsihi H, De Rossi E, Salazar L, Cantoni R, Labo M, Riccardi G, Takiff HE, Eiglmeier K, Bergh S & Cole ST (1996) Gene arrangement and organization in approximately 76 kb fragment encompassing the *ori*C region of the chromosome of *Mycobacterium leprae*. *Microbiology* **142**: 3147–3161.

Horsburg CR Jr (1991) *Mycobacterium avium* complex infection in the acquired immunodeficiency syndrome. *N Engl J Med* **324**: 1332–1338.

Ihira M, Yoshikawa T, Enomoto Y, *et al.* (2004) Rapid diagnosis of human herpesvirus 6 infection by a novel DNA amplification method, loop-mediated isothermal amplification. *J Clin Microbiol* **42**: 140–145.

Iwamoto T, Sonobe T & Hayashi K (2003) Loop-mediated isothermal amplification for direct detection of *Mycobacterium tuberculosis* complex, *M. avium*, and *M. intracellulare* in sputum samples. *J Clin Microbiol* **41**: 2616–2622.

Jamal MA, Maeda S, Nakata N, Kai M, Fukuchi K & Kashiwabara Y (2000) Molecular basis of clarithromycin-resistance in *Mycobacterium avium intracellulare* complex. *Tuberc Lung Dis* **80**: 1–4.

Kasai H, Ezaki T & Harayama S (2000) Differentiation of phylogenetically related slowly growing mycobacteria by their *gyrB* sequences. *J Clin Microbiol* **38**: 301–308.

Kim BJ, Lee SH, Lyu MA, Kim SJ, Bai GH, Chae GT, Kim EC, Cha CY & Kook YH (1999) Identification of mycobacterial species by comparative sequence analysis of the RNA polymerase gene (*rpoB*). *J Clin Microbiol* **37**: 1714–1720.

Kirschner P, Springer B, Vogel U, Meier A, Wrede A, Kiekenbeck M, Bange FC & Bottger EC (1993) Genotypic identification of mycobacteria by nucleic acid sequence determination: report of a 2-year experience in a clinical laboratory. *J Clin Microbiol* **31**: 2882–2889.

Kuboki N, Inoue N, Sakurai T, Di Cello F, Grab DJ, Suzuki H, Sugimoto C & Igarashi I (2003) Loop-mediated isothermal amplification for detection of African trypanosomes. *J Clin Microbiol* **41**: 5517–5524.

Messer W, Blaesing F, Majka J, *et al.* (1998) Functional domains of Dna A proteins. *Biochimie* **81**: 819–825.

Messer W & Weigel C (1997) Dna A initiator – also a transcription factor. *Mol Microbiol* **24**: 1–6.

Metchock BG, Nolte FS & Wallace RJ Jr (1999) *Mycobacterium. Manual of Clinical Microbiology*, 7th edn (Murray PR, Baron EJ, Pfaller MA, Tenover FC & Yolken RH, eds), pp. 399–437. American Society for Microbiology, Washington, DC.

Mizrahi VS, Dawes S & Rubin H (2000) DNA replication. *Molecular Genetics of Mycobacteria* (Hatful GF & Jacobs WR Jr, eds), pp. 159–172. American Society for Microbiology, Washington, DC.

Montessori V, Phillips P, Montaner J, Haley L, Craib K, Bessuille E & Black W (1996) Species distribution in human immunodeficiency virus-related mycobacterial infections: implications for selection of initial treatment. *Clin Infect Dis* **22**: 989–992.

Notomi T, Okayama H, Masubuchi H, Yonekawa T, Watanabe K, Amino N & Hase T (2000) Loop-mediated isothermal amplification of DNA. *Nucleic Acids Res* **28**: E63.

Parida M, Posadas G, Inoue S, Hasebe F & Morita K (2004) Real-time reverse transcription loop-mediated isothermal amplification for rapid detection of West Nile virus. *J Clin Microbiol* **42**: 257–263.

Park H, Jang H, Kim C, Chung B, Chang CL, Park SK & Song S (2000) Detection and identification of mycobacteria by amplification of the internal transcribed spacer regions with genus- and species-specific PCR primers. *J Clin Microbiol* **38**: 4080–4085.

Plikaytis BB, Plikaytis BD, Yakrus MA, Butler WR, Woodley CL, Silcox VA & Shinnick TM (1992) Differentiation of slowly growing *Mycobacterium* species, including *Mycobacterium tuberculosis*, by gene amplification and restriction fragment length polymorphism analysis. *J Clin Microbiol* **30**: 1815–1822.

Primm TP, Lucero CA & Falkinham JO III (2004) Health impacts of environmental mycobacteria. *Clin Microbiol Rev* **17**: 98–106.

Roth A, Fischer M, Hamid ME, Michalke S, Ludwig W & Mauch H (1998) Differentiation of phylogenetically related slowly growing mycobacteria based on 16S–23S rRNA gene internal transcribed spacer sequences. *J Clin Microbiol* **36**: 139–147.

Shepard CC (1960) The experimental diseases that follows the injection of human leprosy bacilli into foot-pads of mice. *J Exp Med* **112**: 445–454.

Springer B, Stockman L, Teschner K, Roberts GD & Bottger EC (1996) Two-laboratory collaborative study on identification of mycobacteria: molecular versus phenotypic methods. *J Clin Microbiol* **34**: 296–303.

Taylor TB, Patterson C, Hale Y & Safranek WW (1997) Routine use of PCR-restriction fragment length polymorphism analysis for identification of mycobacteria growing in liquid media. *J Clin Microbiol* **35**: 79–85.

Telenti A, Marchesi F, Balz M, Bally F, Bottger EC & Bodmer T (1993) Rapid identification of mycobacteria to the species level by polymerase chain reaction and restriction enzyme analysis. *J Clin Microbiol* **31**: 175–178.

Thai HTC, Le MQ, Vuong CD, Parida M, Minekawa H, Notomi T, Hasebe F & Morita K (2004) Development and evaluation of a novel loop-mediated isothermal amplification method for rapid detection of severe acute respiratory syndrome coronavirus. *J Clin Microbiol* **42**: 1956–1961.

Thompson JD, Higgins DG & Gibson TJ (1994) CLUSTAL W: improving the sensitivity of progressive multiple sequence alignment through sequence weighting, position-specific gap penalties and weight matrix choice. *Nucleic Acids Res* **22**: 4673–4680.

Turenne CY, Tschetter L, Wolfe J & Kabani A (2001) Necessity of quality-controlled 16S rRNA gene sequence databases: identifying nontuberculous *Mycobacterium* species. *J Clin Microbiol* **39**: 3637–3648.

Wayne LG & Sramek HA (1992) Agents of newly recognized or infrequently encountered mycobacterial diseases. *Clin Microbiol Rev* **5**: 1–25.

Yang M, Ross BC & Dwyer B (1993) Isolation of a DNA probe for identification of *Mycobacterium kansasii*, including the genetic subgroup. *J Clin Microbiol* **31**: 2769–2772.

Impaired maturation and function of dendritic cells by mycobacteria through IL-1β

Masahiko Makino[1], Yumi Maeda[1], Tetsu Mukai[1] and Stefan H. E. Kaufmann[2]

[1] Department of Microbiology, Leprosy Research Center, National Institute of Infectious Diseases, Tokyo, Japan
[2] Department of Immunology, Max-Planck-Institute for Infection Biology, Berlin, Germany

Dendritic cells (DC) are pivotal for initiation and regulation of innate and adaptive immune responses evoked by vaccination and natural infection. After infection, mycobacterial pathogens first encounter monocytes, which produce pro-inflammatory cytokines, including IL-1β, TNF-α and IL-6. The role of these cytokines in DC maturation remains incompletely understood. Here, we show that maturation of DC from monocytes was impaired by pretreatment of monocytes with low doses of IL-1β. Under these conditions, *Mycobacterium leprae*-infected DC failed to stimulate antigen-specific T cell responses. Expression of CD86 and CD83 and production of IL-12 in response to lipopolysaccharide and peptidoglycan were diminished. In contrast, these DC functions were not impaired by pretreatment with TNF-α, IL-6 or IL-10. When monocytes were infected with *M. bovis* Bacillus Calmette-Guérin, and subsequently differentiated to DC, the activity of these DC was suppressed as well. Thus, IL-1β acts at early stages of differentiation of DC and impairs biological functions of DC at later stages. Therefore, production of IL-1β by mycobacteria-infected antigen-presenting cells counteracts effective stimulation of innate and adaptive immune responses.

Received 29/11/05
Revised 25/2/06
Accepted 10/3/06

[DOI 10.1002/eji.200535727]

Key words:
BCG · Dendritic cell · IL-1β · IL-12

Introduction

Infections by mycobacterial pathogens still cause major health problems globally. *Mycobacterium tuberculosis* kills more adults than any other infectious agent and one third of the world's population is considered infected with this pathogen [1, 2]. *M. leprae* affects skin and peripheral nerves, causing massive body deformation [3, 4]. These pathogenic mycobacteria persist *in vivo* over long periods without being eradicated by the host immune system [5]. The current vaccine against tuberculosis, BCG has only limited protective effects, and no reliable vaccine has been developed against leprosy [6, 7].

Host defense against mycobacteria in human is primarily conducted by type 1 adaptive immune responses, and DC play a major role as APC [8, 9]. To elicit T cell immunity, activation of APC is critical and strongly influenced by pro-inflammatory cytokines [10–12]. Type 1 $CD4^+$ T cells are stimulated by cognate interactions with APC and IL-12 costimulation [13]. IL-12 is preferentially produced by activated DC and its production is associated with the activation of NF-κB [14, 15]. After appropriate stimulation, blood monocytes can mature to DC and 25% of the circulating inflammatory monocytes are estimated to differentiate to DC and 75% to tissue macrophages [16, 17]. Resting

Correspondence: Dr. Masahiko Makino, Department of Microbiology, Leprosy Research Center, National Institute of Infectious Diseases, 4-2-1 Aobacho, Higashimurayama, Tokyo 189–0002, Japan
Fax: +81-42-391-8212
e-mail: mmaki@nih.go.jp

Abbreviations: MLC: *M. leprae*-derived cytosolic fraction · **MMP:** major membrane protein · **PGN:** peptidoglycan

macrophages serve as habitat for mycobacteria [18]. After infection with mycobacteria, mononuclear phagocytes rapidly produce cytokines including IL-1β as first-line mediators of defense [5, 19].

IL-1β is a 17-kDa prototypic pro-inflammatory cytokine. IL-1β is multifunctional and acts on a wide variety of target cells [20]. It induces numerous genes regulated by IL-1β-inducible transcription factors such as NF-κB [21, 22]. Therefore, IL-1β not only participates in the innate immune response, but also influences T cell activity. However, the effect of IL-1β on monocytes undergoing differentiation into DC remains unknown especially with regard to the adaptive T cell response against mycobacteria.

Here, we show that IL-1β in picomolar quantities markedly influences monocyte maturation to DC with profound consequences for subsequent T cell responses. Our findings that mycobacteria impair DC differentiation and function via IL-1β can explain at least partially the persistence of mycobacteria in host cells.

Results

Effects of IL-1β pretreatment of monocytes on DC-mediated T cell stimulation

Monocytes primed with BCG produced significant concentrations of IL-1β at MOI ≥0.06 (Table 1). Similarly, macrophages produced IL-1β in response to priming with BCG although less efficiently than monocytes. These findings raised the question whether IL-1β influences maturation of DC from monocytes.

To this end, we pretreated monocytes with IL-1β and then allowed them to mature into DC (Table 2). DC derived from untreated monocytes stimulated $CD4^+$ T cells after a pulse with *M. leprae* (MOI 20). In contrast, $CD4^+$ T cell stimulation by DC differentiated from IL-1β pretreated monocytes was markedly impaired. Inhibition depended on the IL-1β concentration used for pretreatment of monocytes. Significant inhibition was achieved at ≥ 100 pg/mL IL-1β. Similarly, IL-1β inhibited T cell stimulation when other Ag, including heat-killed *M. leprae* or major membrane protein (MMP)-II were used to pulse DC. IL-4 or IL-10 were not produced by $CD4^+$ T cells under these conditions (data not shown). IL-1α impaired APC functions of DC in a similar manner as IL-1β, whereas other pro-inflammatory cytokines, including TNF-α and IL-6 did not affect Ag-presenting functions of DC.

Phenotype of DC derived from IL-1β-pretreated monocytes

In an attempt to characterize DC derived from IL-1β-pretreated monocytes, we determined surface markers of immature DC (Fig. 1). Immature DC derived from monocytes, which had been pretreated with IL-1β or not, expressed similar or mildly reduced cell surface levels of HLA-ABC, HLA-DR and CD1a, and were devoid of the macrophage marker CD14. Similarly, the ability of immature DC to engulf mycobacteria as assessed by uptake of GFP-expressing BCG did not differ significantly (GFP-expressing *M. leprae* could not be prepared because of the inability of this obligate intracellular pathogen to grow *in vitro*). Subsequently, we determined surface markers of mature DC generated by LPS stimulation (Fig. 2). Expression of HLA-ABC and HLA-DR was not significantly altered by IL-1β pretreatment of monocytes. In contrast, CD86 and CD83 were down-regulated by IL-1β pretreatment, both with respect to surface expression and percent of positive cell numbers (Fig. 2A). These phenotypic alterations were also observed with *M. leprae*-infected mature DC (data not shown). IL-1β did not influence the surface expression of MMP-II, one of the dominant Ag of *M. leprae* [23], on *M. leprae*-pulsed mature DC (Fig. 2B). In addition, IL-1β or BCG pretreatment of monocytes did not alter the expression of TLR2 and TLR4 (Fig. 2C). Finally, IL-1β pretreatment of monocytes did not cause apoptosis of DC (data not shown). Thus, DC differentiated from IL-1β pretreated monocytes were only partially activated.

Table 1. IL-1β production after stimulation of mononuclear phagocytes with BCG[a)]

Cell type	IL-1β (pg/mL) production after stimulation with BCG at MOI:			
	0	0.0625	0.25	1.0
Monocytes	2.2 ± 0.2	23.7 ± 4.6*[b)]	229.4 ± 19.1**[b)]	861.4 ± 22.3***[b)]
Macrophages	3.3 ± 0.4	4.0 ± 1.1	34.6 ± 2.8**	163.3 ± 20.1****[b)]

a) Plastic adherent monocytes, and M-CSF (5 ng/mL)-treated macrophages (1×10^5/well) were stimulated for 24 h with BCG at the indicated MOI. Assays were done in triplicate, and results are expressed as mean ± SD.

b) $^{*}p < 0.05$ *vs.* control (MOI 0), $^{**}p < 0.005$ *vs.* control (MOI 0), $^{***}p < 0.0005$ vs. control (MOI 0), $^{****}p < 0.01$ *vs.* control (MOI 0).

Table 2. *M. leprae*-specific IFN-γ production by $CD4^+$ T cells stimulated by *M. leprae*-pulsed DC derived from IL-1β pretreated monocytes[a)]

IL-1β pretreatment of monocytes (pg/mL)	*M. leprae* infection of immature DC (MOI)	IFN-γ (pg/mL) secretion by $CD4^+$ T cells after stimulation with DC at ratio (T: DC):	
		20:1	40:1
0	0	0.7 ± 0.0	0.2 ± 0.0
0	20	206.7 ± 15.1	50.7 ± 4.9
30	0	0.4 ± 0.0	0.3 ± 0.1
30	20	192.8 ± 19.3	24.9 ± 11.2
100	0	0.3 ± 0.1	0.6 ± 0.2
100	20	50.9 ± 6.1*[b)]	13.4 ± 0.3*
300	0	0.7 ± 0.4	0.8 ± 0.7
300	20	30.3 ± 2.6*	9.7 ± 1.9**[b)]
1000	0	0.3 ± 0.1	0.4 ± 0.2
1000	20	9.5 ± 2.1*	3.0 ± 0.5*

[a)] $CD4^+$ T cells (1×10^5/well) were stimulated for 4 days with autologous DC at the indicated T cell:DC ratio. Immature DC differentiated from untreated or IL-1β-treated monocytes were pulsed with *M. leprae* on day 3, treated with LPS (25 ng/mL) on day 4, and were used as APC on day 5. Representative data of three separate experiments are shown. Assays were done in triplicate, and results are expressed as mean ± SD.

[b)] *$p < 0.0001$ *vs.* control (IL-1β 0 pg/mL, *M. leprae* (MOI 20)), **$p < 0.0005$ *vs.* control (IL-1β 0 pg/mL, *M. leprae* (MOI 20)).

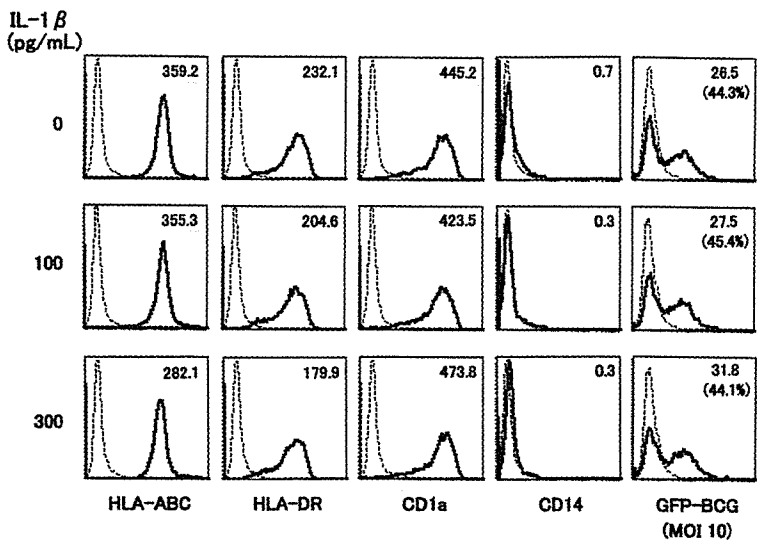

Figure 1. Phenotype and phagocytic activity of immature DC differentiated from IL-1β pretreated monocytes. Plastic adherent monocytes were pretreated with the indicated doses of IL-1β and were subsequently differentiated into DC by 3-day culture with rGM-CSF and rIL-4. For analysis of phagocytic activity of DC, the immature DC (cultured for 3 days) were pulsed with GFP-expressing BCG (MOI 10) and expression of GFP was assessed on day 4 of culture. Dashed lines, isotype-matched control IgG; solid lines, mAb staining. The number represents the difference in mean fluorescence intensity between dotted and solid lines. The number in parentheses indicates percent positive cell number. Representative data of three independent experiments are shown.

Effects of IL-1β pretreatment of monocytes on IL-12 production by DC

In order to determine whether DC differentiated from IL-1β pretreated monocytes can be adequately activated, we determined IL-12p70 production by DC in response to TLR2 and TLR4 signaling. DC obtained on day 4 of culture were found optimal for stimulation by the TLR4 ligand LPS and the TLR2 ligand peptidoglycan (PGN) (data not shown). DC derived from untreated monocytes produced IL-12p70 in response to LPS in a dose-dependent manner, whereas DC differentiated from monocytes pretreated with IL-1β failed to produce significant amounts of IL-12 (Fig. 3A). Similar results

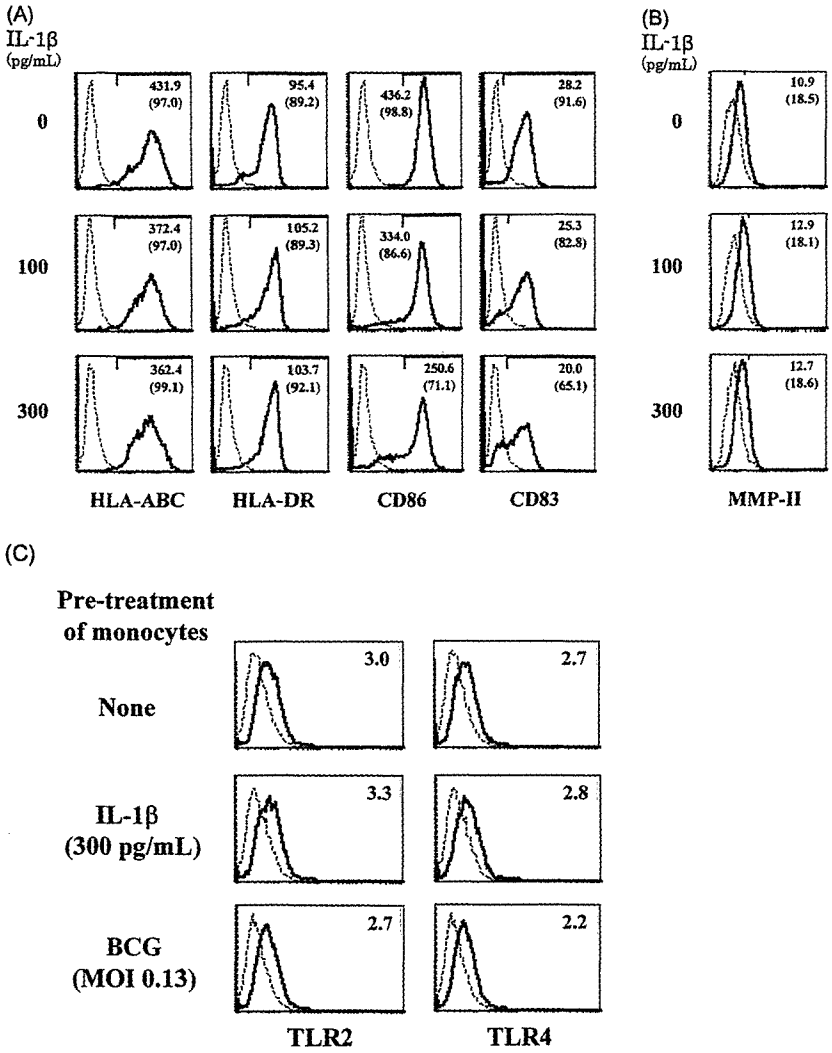

Figure 2. (A) Phenotype of mature DC differentiated from monocytes pretreated with IL-1β. Plastic adherent monocytes were pretreated with the indicated doses of IL-1β and were subsequently differentiated into DC by 5-day culture with rGM-CSF and rIL-4. Cells were treated with LPS (25 ng/mL) on day 4 and analyzed on day 5. Dashed lines, isotype-matched control IgG; solid lines, mAb staining. The number represents the difference in mean fluorescence intensity between dotted and solid lines. The number in parentheses indicates percent positive cell number. Representative data of three independent experiments are shown. (B) MMP-II expression on mature DC obtained as in (A), except that DC were infected with *M. leprae* (MOI 20) on day 3. Dashed lines, isotype-matched control IgM; solid lines, mAb staining. The number represents the difference in mean fluorescence intensity between dotted and solid lines. The number in parentheses indicates percent positive cell number. Representative data of three independent experiments are shown. (C) Expression of TLR on mature DC differentiated from monocytes pretreated with IL-1β or BCG. Plastic adherent monocytes were pretreated with the indicated doses of IL-1β or BCG and were subsequently differentiated into mature DC as in (A). Dashed lines, isotype-matched control IgG; solid lines, mAb staining. The number represents the difference in mean fluorescence intensity between dotted and solid lines. Representative data of three independent experiments are shown.

were obtained for TNF-α production by DC (data not shown). Moreover, untreated DC produced IL-12p70 in response to PGN in a dose-dependent manner, whereas IL-1β pretreatment of monocytes significantly impaired IL-12p70 production (Fig. 3B) although expression of TLR2 on the surface of DC was not altered under these conditions (data not shown). IL-12p70 production in response to MMP-II, which ligates to TLR2, was similarly affected by pretreatment of monocytes with IL-1β (Fig. 3C). Also, both rIL-1β (Fig. 3D) and BCG (Fig. 3E) induced IL-12p70 production only in DC derived from IL-1β untreated-monocytes. The failure to produce IL-12p70 was long lasting as DC differentiated from IL-1β pretreated monocytes in the presence of GM-CSF and IL-4 did not produce IL-12p70 in response to LPS for up to 7 days (data not shown). Next, we examined whether other cytokines produced by monocytes infected with BCG inhibited IL-12 production by DC. Monocytes were pretreated with 100 pg/mL of TNF-α, IL-6 or IL-10, differentiated to DC, which were then stimulated with LPS. None of these cytokines impaired IL-12p70 secretion by DC (Table 3). Thus, IL-1β signaling in monocytes but not IL-6, TNF-α or IL-10 signaling, inhibited IL-12 secretion by DC. Subsequently, IL-1β sensitivity of monocytes undergoing DC maturation was determined. Monocytes were cultured for 3 days in the presence of rGM-CSF and rIL-4 and then treated with IL-1β or other cytokines and 24 h later stimulated with LPS. Cells treated with TNF-α or IL-6 produced similar concentrations of IL-12p70 as compared to untreated DC in response to LPS. In contrast, IL-1β treatment significantly reduced IL-12p70 production (Table 4).

Effects of endogenous IL-1β on IL-12p70 production by DC

We assessed the influence of endogenously produced IL-1β on IL-12p70 production by DC (Table 5). The *M. leprae*-derived cytosolic protein (MLC preparation), which represents an antigenic fraction, did not induce IL-1β production in monocytes at concentrations up to

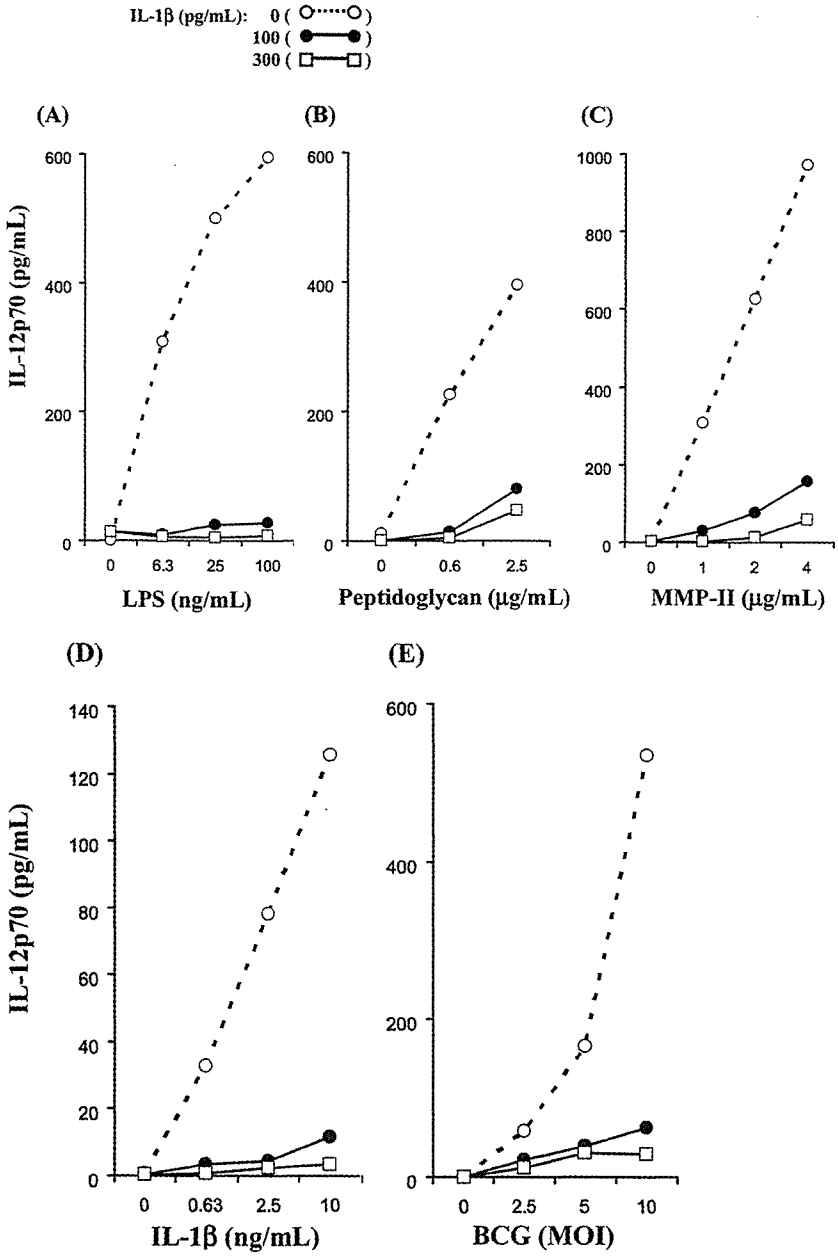

Figure 3. IL-12p70 production by stimulated mature DC. DC were differentiated by 4-day culture with rGM-CSF and rIL-4 from monocytes. Monocytes were treated with the indicated doses of rIL-1β (○----○: IL-1β 0, ●—●: IL-1β 100 and □—□: IL-1β 300 pg/mL), and were stimulated for 24 h with: (A) LPS, (B) PGN, (C) MMP-II, (D) IL-1β and (E) BCG at indicated doses. IL-12p70 concentrations were measured by ELISA. Representative data of three independent experiments are shown.

1 μg/mL, whereas 1 pg/mL LPS stimulated IL-1β secretion in monocytes. Accordingly, DC derived from monocytes pretreated with MLC produced equal concentrations of IL-12p70 as untreated DC did, whereas DC derived from LPS pretreated monocytes failed to secrete significant concentrations of IL-12p70. Monocytes infected with BCG at MOI <0.03 did not produce significant levels of IL-1β and accordingly were able to produce IL-12p70 after differentiation into DC. In contrast, BCG at MOI 0.13 stimulated IL-1β production from monocytes and concomitantly inhibited IL-12p70 secretion by DC. BCG infection did not cause apoptosis under these conditions (data not shown). To directly determine the role of endogenous IL-1β on IL-12 production by DC, antibody neutralization experiments were performed (Table 6). DC derived from BCG-pretreated monocytes were significantly impaired in IL-12p70 production and this impairment was abrogated when neutralizing IL-1β mAb were present during BCG pretreatment. Control mAb showed no neutralizing effects. In addition, impaired IL-12p70 production by LPS pretreated monocytes was abrogated by neutralizing mAb to IL-1β (not shown). Thus, BCG inhibited IL-12 production by DC via IL-1β signaling in monocytes.

Discussion

Host defense against mycobacterial pathogens is mediated by innate and adaptive immune responses.

Table 3. IL-12p70 production by DC differentiated from monocytes pretreated with various cytokines[a)]

Cytokine pretreatment of monocytes (100 pg/mL)	IL-12p70 (pg/mL) production by DC after stimulation with LPS at dose:		
	0	6.3 ng/mL	25 ng/mL
None	4.7 ± 0.8	363.4 ± 6.2*[b)]	546.7 ± 8.7*
IL-1β	3.4 ± 1.0	18.0 ± 2.2*	48.0 ± 5.1*
TNF-α	3.8 ± 0.8	352.8 ± 5.8	531.5 ± 7.3
IL-6	4.0 ± 0.4	375.2 ± 9.8	564.4 ± 11.8
IL-10	1.3 ± 0.1	400.3 ± 11.9	895.8 ± 29.9

a) DC (1×10^5/well) were differentiated from monocytes pretreated with either of the above cytokines on day 0 of culture. On day 4 of culture, DC were stimulated with LPS for 24 h. Representative data of three separate experiments are shown. Assays were done in triplicate, and results are expressed as mean ± SD.

b) *$p < 0.0001$ *vs.* control (LPS 0 ng/mL).

Table 4. Effects of cytokine pretreatment on IL-12p70 production by DC[a)]

Cytokine pretreatment of immature DC (100 pg/mL)	IL-12p70 production (pg/mL) by DC after stimulation with LPS at dose:		
	0	6.3 ng/mL	25 ng/mL
None	0.2 ± 0.0	333.9 ± 11.0*[b)]	539.2 ± 20.3*
IL-1β	0.3 ± 0.0	68.5 ± 9.8*	219.1 ± 10.7*
TNF-α	8.4 ± 1.9	330.7 ± 12.8	534.1 ± 30.0
IL-6	3.6 ± 0.8	331.8 ± 13.4	535.9 ± 29.2

a) Monocytes cultured for 3 days in the presence of rGM-CSF and rIL-4 (1×10^5/well) were pretreated with cytokines and on day 4 cells were further stimulated with LPS for 24 h. Representative data of three separate experiments are shown. Assays were done in triplicate, and results are expressed as mean ± SD.

b) *$p < 0.0005$ *vs.* control (LPS 0 ng/mL).

Table 5. IL-12p70 production by DC derived from Ag-pulsed monocytes[a)]

	Monocyte treatment	IL-1β production (pg/mL) by monocytes[b)]	IL-12p70 production (pg/mL) by DC after stimulation with LPS at dose:		
			0	6.3 ng/mL	25 ng/mL
Exp. 1	None	1.3 ± 0.1	11.8 ± 2.1	250.8 ± 18.7	489.9 ± 21.0
	MLC[c)] (1 μg/mL)	1.6 ± 0.2	13.3 ± 1.8	224.1 ± 17.9	360.9 ± 15.4
	LPS (1 pg/mL)	150.3 ± 3.9	4.0 ± 0.9	1.8 ± 0.3*[d)]	1.5 ± 0.1**
	MLC[c)] (1 μg/mL) + LPS (1 pg/mL)	160.8 ± 4.3	4.4 ± 0.8	0.9 ± 0.2*	0.0 ± 0.0**[d)]
Exp. 2	None	0.0 ± 0.1	0.0 ± 0.0	309.6 ± 20.5	499.3 ± 23.7
	BCG (MOI 0.03)	6.8 ± 0.7	14.6 ± 2.6	264.7 ± 21.8	493.2 ± 21.8
	BCG (MOI 0.13)	148.7 ± 9.6	5.0 ± 1.1	44.6 ± 3.9*	91.8 ± 12.3**

a) DC (1×10^5/well) were derived from monocytes pulsed with Ag or LPS. DC were then stimulated for 24 h with LPS. Representative data of three separate experiments are shown. Assays were done in triplicate, and results are expressed as mean ± SD.

b) The concentration of IL-1β produced by monocytes after priming with indicated stimulator.

c) MLC: *M. leprae*-derived cytosol fraction.

d) *$p < 0.005$ *vs.* None (Monocyte not pretreated), **$p < 0.001$ *vs.* None (Monocyte not pretreated).

